

## THE INCLINATION ANGLE AND MASS OF THE BLACK HOLE IN XTE J1118+480

DAWN M. GELINO

Michelson Science Center, California Institute of Technology, MS 100-22, 770 South Wilson Avenue, Pasadena,  
CA 91125; dawn@ipac.caltech.edu

ŞÖLEN BALMAN, ÜMIT KIZILOĞLU, AND ARDA YILMAZ  
Middle East Technical University, Ankara, Turkey

EMRAH KALEMCI

Sabancı University, Orhanlı-Tuzla, Istanbul, 34956, Turkey

AND

JOHN A. TOMSICK

Center for Astrophysics and Space Sciences, Code 0424, University of California at San Diego, La Jolla, CA 92093

Received 2005 September 20; accepted 2006 January 2

### ABSTRACT

We have obtained optical and infrared photometry of the quiescent soft X-ray transient XTE J1118+480. In addition to optical and  $J$ -band variations, we present the first observed  $H$ - and  $K_s$ -band ellipsoidal variations for this system. We model the variations in all bands simultaneously with the WD98 light curve modeling code. The infrared colors of the secondary star in this system are consistent with a spectral type of K7 V, while there is evidence for light from the accretion disk in the optical. Combining the models with the observed spectral energy distribution of the system, the most likely value for the orbital inclination angle is  $68^\circ \pm 2^\circ$ . This inclination angle corresponds to a primary black hole mass of  $8.53 \pm 0.60 M_\odot$ . Based on the derived physical parameters and infrared colors of the system, we determine a distance of  $1.72 \pm 0.10$  kpc to XTE J1118+480.

*Subject headings:* binaries: close — infrared: stars — stars: individual (XTE J1118+480) — stars: variables: other — X-rays: binaries

### 1. INTRODUCTION

Transient low-mass X-ray binaries (LMXBs) exhibit large and abrupt X-ray and optical outbursts that can be separated by decades of quiescence (Chen et al. 1997). For these systems, the compact object is a black hole or a neutron star, and the companion is normally a low-mass K- or M-type dwarflike star (Charles & Coe 2006). During their periods of quiescence, these systems are faint at X-ray, optical, and infrared (IR) wavelengths. While the quiescent X-ray emission can be caused by accretion onto a compact object or thermal emission from the surface of a neutron star (Garcia et al. 2001; Wijnands 2005), the companion can dominate the luminosity at optical and IR energies. During the binary orbit, the changing aspect of the tidally distorted companion causes a periodic modulation of the optical and IR emission (Gelino 2001). Measurements of these “ellipsoidal variations” provide information about the physical parameters of the binary.

XTE J1118+480 ( $\alpha_{2000} = 11^{\text{h}}18^{\text{m}}10^{\text{s}}.85$ ,  $\delta_{2000} = 48^\circ 02' 12.9''$ ) was discovered with the all-sky monitor (ASM) on the *Ross X-Ray Timing Explorer* by Remillard et al. (2000) on 2000 March 29, while Garcia et al. (2000) spectroscopically identified its 12.9 mag optical counterpart. Owing to its position in the Galactic halo, this high-latitude ( $b = +62^\circ$ ) system has been observed by numerous groups over many wavelength regimes. Recent orbital parameters determined from optical spectra suggest an orbital period of 4.078 hr and a secondary star radial velocity semiamplitude of  $709 \pm 7$  km s $^{-1}$  (Torres et al. 2004). These values imply a mass function of  $f(M) = 6.3 \pm 0.2 M_\odot$ , identifying the compact object as a black hole.

Determining a precise black hole mass requires an accurate measurement of the orbital inclination angle of the system. As discussed in Gelino et al. (2001b), the best way to find the in-

clination angle in a noneclipsing system is to model its infrared ellipsoidal light curves. In the IR regime, there is a smaller chance of contamination from other sources of light in the system. While modeling several light curves from one wavelength regime helps to constrain model parameters, simultaneously modeling light curves that span more than one wavelength regime provides tighter constraints than modeling IR light curves alone. Previous inclination estimates for XTE J1118+480 have come from modeling optical ellipsoidal variations as the system approached quiescence (McClintock et al. 2001; Wagner et al. 2001; Zurita et al. 2002b). These inclination angles range from  $55^\circ$  (McClintock et al. 2001) to  $83^\circ$  (Wagner et al. 2001), and correspond to primary masses of 10 and  $6.0 M_\odot$ , respectively. Since this system has been known to exhibit optical superhumps from the precession of an eccentric accretion disk on its way to quiescence (Zurita et al. 2002b), it is important to determine the orbital inclination angle while XTE J1118+480 is in a truly quiescent state.

In order to determine an accurate orbital inclination angle for XTE J1118+480, we have obtained  $B$ -,  $V$ -,  $R$ -,  $J$ -,  $H$ -, and  $K_s$ -band light curves of the system while in quiescence, and simultaneously model them here with the WD98 light curve modeling code (Wilson 1998). To date, this is the most comprehensive ellipsoidal variation data set published for this system. The modeled inclination angle is combined with recently published orbital parameters to determine a highly constrained mass of the black hole in this X-ray binary.

### 2. OBSERVATIONS AND DATA REDUCTION

We observed the XTE J1118+480 field in the optical and IR wavelength regimes. Table 1 summarizes our observations, and we describe them in detail below.

TABLE 1  
OBSERVATIONS OF XTE J1118+480

Date	Filter	Exposure Time <sup>a</sup>	Percent Orbital Coverage
2003 Jan 17.....	<i>J, H, K<sub>s</sub></i>	200	179
2003 Jan 18.....	<i>J, H, K<sub>s</sub></i>	200	172
2003 Jun 4.....	<i>V, R</i>	240	14 <sup>b</sup> , 9 <sup>c</sup>
2003 Jun 5.....	<i>V, R</i>	240	62 <sup>b</sup> , 73 <sup>c</sup>
2003 Jun 6.....	<i>V, R</i>	240	44 <sup>b</sup> , 40 <sup>c</sup>
2004 Mar 18.....	<i>V</i>	300	192
2004 Mar 19.....	<i>R</i>	300	224
2004 Apr 23.....	<i>B</i>	420	28
2004 Apr 24.....	<i>B</i>	420	83

<sup>a</sup> Effective exposure time per image in seconds.

<sup>b</sup> Orbital coverage percentage for the *V* filter.

<sup>c</sup> Orbital coverage percentage for the *R* filter.

### 2.1. Optical Observations

We obtained optical observations of XTE J1118+480 over three nights in 2003 and four nights in 2004 using standard Johnson *B*, *V*, and *R* filters with the 1.5 m telescope at the TÜBİTAK National Observatory (TUG)<sup>1</sup> in Antalya, Turkey. The data were obtained with the imaging CCD<sup>2</sup> on 2003 June 4–6 and the ANDOR CCD<sup>3</sup> on 2004 March 18–19 and 2004 April 23–24. A total of 31, 84, and 83 images were obtained in the *B*, *V* and *R* bands, respectively. The data were reduced with bias frames, dark-current frames, and dome flat fields using standard procedures. The instrumental magnitudes of XTE J1118+480 were derived through the use of the point-spread function (PSF)-fitting algorithms, DAOPHOT (Stetson 1987) and ALLSTAR in the MIDAS software package using 15 PSF stars. In addition, a reference star ( $\alpha = 11^{\text{h}}18^{\text{m}}07^{\text{s}}.10$ ,  $\delta = +48^{\circ}03'53''.2$ ) close to our transient source was used to reduce the scintillation effects and derive the calibrated magnitudes for a given filter. The reference star and target star errors were added in quadrature to produce the final errors on the photometric points. The resulting data were combined into 20 bins per orbit.

### 2.2. Infrared Observations

Infrared data on XTE J1118+480 were obtained on 2003 January 17 and 18 using SQUID (simultaneous quad infrared imaging device)<sup>4</sup> on the 2.1 m telescope at Kitt Peak National Observatory. We simultaneously obtained measurements in the *J*, *H*, and *K<sub>s</sub>* bands and kept the number of counts in each exposure in the linear regime of each chip. The data were reduced using tasks in the `upsquid` package in IRAF.<sup>5</sup> The images taken at one position were subtracted from the images taken at a slightly offset position to remove the sky, dark current, and any bias level. We then flat-fielded the images using twilight sky flats.

Aperture photometry was performed on XTE J1118+480 and five nearby field stars. Using the IRAF phot package, a differential light curve for each band was generated. We followed standard error propagation rules for calculating the differential magnitude errors from the target and reference star instrumental magnitudes. The differential photometric results show that over the course of our observations, the comparison stars did not

<sup>1</sup> See <http://www.tug.tubitak.gov.tr/index.html?en>.

<sup>2</sup> See [http://www.tug.tubitak.gov.tr/aletler/SDSU\\_imaging\\_ccd/](http://www.tug.tubitak.gov.tr/aletler/SDSU_imaging_ccd/).

<sup>3</sup> See <http://hea.iki.rssi.ru/AZT22/ENG/focal.htm>.

<sup>4</sup> See <http://www.noao.edu/kpno/squid/>.

<sup>5</sup> IRAF is distributed by the National Optical Astronomy Observatories, which are operated by the Association of Universities for Research in Astronomy, Inc., under cooperative agreement with the National Science Foundation.

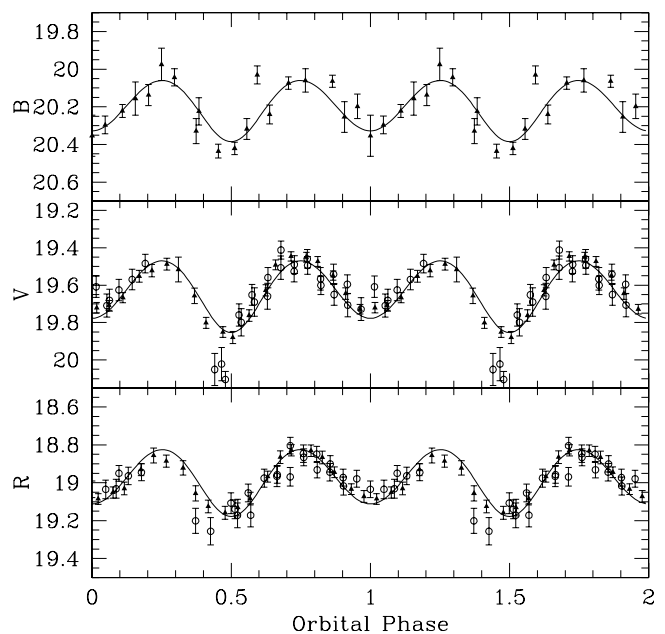


FIG. 1.—XTE J1118+480 *B*-, *V*-, and *R*-band light curves from 2003 (*open circles*) and 2004 (*filled triangles*). The data are plotted over two phase cycles for clarity. Error bars are  $1\sigma$ . The solid line represents the best-fitting ( $i = 68^\circ$ ) WD98 model as described in the text.

vary more than expected from photon statistics. We used photometric images of the Hunt et al. (1998) AS-11 and AS-18 ARNICA standard star fields, as well as 2MASS field stars, to calibrate the data set. As with the optical, the data were combined into 20 bins per orbit.

## 3. RESULTS AND DISCUSSION

Figure 1 presents the resulting *B*-, *V*-, and *R*-band light curves of XTE J1118+480, while the final *J*, *H*, and *K<sub>s</sub>* differential light curves are presented in Figure 2. Despite the expectation of detecting superhumps from the 52 day accretion disk precession

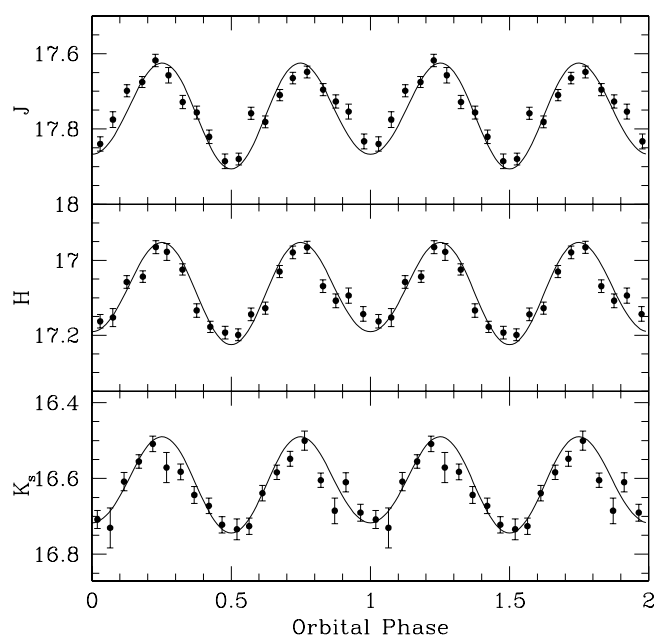


FIG. 2.—XTE J1118+480 *J*-, *H*-, and *K<sub>s</sub>*-band light curves (*circles*). The data are plotted over two phase cycles for clarity. Error bars are  $1\sigma$ . The solid line represents the best-fitting ( $i = 68^\circ$ ) WD98 model as described in the text.

period, there was no evidence of a superhump period when the data were run through a periodogram. These results are consistent with the findings of Shahbaz et al. (2005), whose optical data taken in 2003 June suggested that if a superhump modulation existed, it was at the  $<0.50\%$  level. Shahbaz et al. (2005) also observed stochastic variability and fast flares in their light curves. However, the observed stochastic variability had the same magnitude as their photometric error bars, and despite the significant power in the power density spectrum, the flares seen in XTE J1118+480 had roughly the same magnitude as the spread in the comparison star measurements. The 2003 and 2004  $V$ - and  $R$ -band light curves presented here were consistent in shape and amplitude. As Table 1 shows, on two-thirds of the nights that XTE J1118+480 was observed, data were gathered for at least 75% of an orbit, with more than one full orbit covered on four of the nine nights. No evidence for unequal maxima, flares, or light-curve distortions were found in the unphased data. The periodogram results are consistent with the results from Torres et al. (2004), and therefore, all data presented here have been phased to their ephemeris. These are the first  $H$ - and  $K_s$ -band detections of ellipsoidal variations from this X-ray binary system.

### 3.1. Ellipsoidal Models

The spectral type of the secondary star can be estimated by comparing its red optical spectrum with the spectra of stars with various spectral types from the same luminosity class. Alternatively, one can use a spectral energy distribution (SED) and published limits on the spectral type to not only derive an effective temperature of the secondary star, but also estimate both the visual extinction and contamination level. Given that photometric data usually have a higher signal-to-noise ratio (S/N) than spectroscopic data, an effective temperature derived using photometry can be just as useful as a spectral type derived from a spectroscopic data set. To this end, we compared the observed optical/IR ( $BVRJHK_s$ ) SED for XTE J1118+480 with the observed SEDs for K0 V–M4 V stars (Bessell & Brett 1988; Bessell 1991; Mikami & Heck 1982). We present the best-fitting SED in Figure 3 and find that it predicts a visual extinction of  $A_V = 0.065 \pm 0.020$  mag and a secondary star spectral type of K7 V. It also includes 60%–70% light from the accretion disk at  $B$  and 30%–35% at  $V$ . A K5 V gives a slightly worse fit, and predicts more  $R$ -band light than is observed, as well as a smaller amount of disk light in the  $B$  and  $V$  bands, inconsistent with previously published values. The visual extinction found here is consistent with the column density adopted by McClintock et al. (2004),  $N_H = 1.2 \times 10^{20} \text{ cm}^{-2}$ , based on three independent measurements, and the spectral type found here is consistent with those found through spectral fitting (K5/7 V; McClintock et al. 2003; Torres et al. 2004).

Light from the primary object or accretion disk in an X-ray binary will act to dilute the amplitude of the ellipsoidal variations of the secondary star. Torres et al. (2004) estimate that the secondary star in the XTE J1118+480 system contributes roughly 55% of the total flux between 5800 and 6400 Å; however, at  $R = 18.6$  mag, the system was not in true quiescence when their observations were taken. Zurita et al. (2002a) determined that XTE J1118+480 has a true quiescent  $R$ -band magnitude of 18.9. The optical data presented here ( $R = 19.00$  mag) are consistent with this value, and thus we contend that the system was in a quiescent state during our observations. In addition, Doppler imaging of the system did not detect any  $H\alpha$  emission from a hot spot or accretion stream (Torres et al. 2004). Since our observations took place while XTE J1118+480 was in true quiescence, the optical data presented here are consistent with both of the Torres et al. (2004) results.

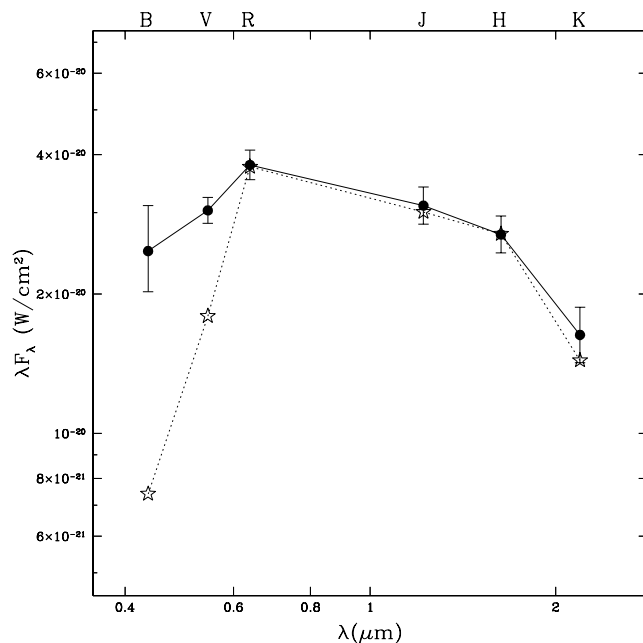


FIG. 3.—XTE J1118+480 phase-averaged optical-infrared quiescent SED dereddened by  $A_V = 0.065$  mag (filled circles). Error bars are  $1\sigma$ . The observed data were compared with SEDs for K0 V–M4 V stars with  $A_V = 0.045$ – $0.085$  mag. The best-fit SED, normalized at  $H$ , is that of a K7 V with 65% extra light at  $B$  and 33% extra light at  $V$  (open stars).

The most difficult contamination source to extract in the case of XTE J1118+480 is the one that has the shallowest spectral slope. If the disk contamination in the infrared is based on the assumption that the optically thin disk radiates through free-free emission processes, and we therefore ascribe the entire  $V$ -band excess to free-free emission, then in the  $K_s$  band, the contamination would be  $\sim 8\%$ . An 8% contamination in the infrared bands would cause the observed orbital inclination angle of the system to be underestimated by  $2^\circ$ . What if we instead assume that any IR contamination is ascribed to a jet or some form of an advection-dominated accretion flow (ADAF)? Models by Yuan & Cui (2005) for XTE J1118+480 in quiescence show that both the jet and ADAF flux in the IR are predicted to constitute significantly less than 8% of the companion flux.

Irradiation of the secondary star by the accretion disk will affect the symmetry of the ellipsoidal light curves. Torres et al. (2004) investigated the possibility of X-radiation powering the  $H\alpha$  emission seen in their Doppler tomograms of the XTE J1118+480 system. They concluded that it was improbable that this could be the case and found that the strength of the  $H\alpha$  emission from the secondary star was comparable with other K dwarfs. Similarly, we see no significant evidence for irradiation effects in the unphased data or the light curves presented here.

As in Gelino et al. (2001b), we simultaneously modeled the optical and infrared light curves of XTE J1118+480 with WD98 (Wilson 1998). See Gelino et al. (2001a) for references and a basic description of the code, and Gelino (2001) for a more comprehensive description.

The data were run through WD98's DC routine, which uses a Simplex algorithm for initial parameter searches and a damped least-squares algorithm for error minimization between the data and model light curves. We ran the code for a semidetached binary with the primary component's gravitational potential set so that all of its mass is concentrated at a point. The most important wavelength-independent input values to WD98 are listed in Table 2. The models were run for a range of inclination angles

TABLE 2  
WAVELENGTH-INDEPENDENT WD98 INPUT PARAMETERS

Parameter	Value
Orbital period (days).....	0.1699339
Ephemeris (HJD phase 0.0) <sup>a</sup> .....	2,451,880.1086
Orbital eccentricity.....	0.0
Temperature of secondary (K).....	4250
Mass ratio ( $M_2/M_1$ ).....	0.0435
Atmosphere model.....	Kurucz (log $g = 4.59$ )
Limb-darkening law.....	Square root
Secondary star gravity-darkening exponent.....	$\beta_1 = 0.34$
Secondary star bolometric albedo.....	0.676

<sup>a</sup> From Torres et al. (2004).

with parameters for a K3 V through an M1 V secondary star. The secondary star atmosphere was determined from solar-metallicity Kurucz models. We used normal, nonirradiated, square-root limb-darkening coefficients (van Hamme 1993). We also adopted gravity-darkening exponents found by Claret (2000) and mass ratios ranging from  $q = 0.030$  to  $0.056$  (Harlaftis et al. 1999; Orosz 2001). We assumed that the secondary star was not exhibiting any star spots during our observations. The models were run with varying amounts of additional light in all bands. Solving for six consistent light curve solutions simultaneously allowed the rejection of many disk light scenarios.

With 118 degrees of freedom, the best-fit model had a reduced  $\chi^2$  of 1.65. While the error on the best-fit inclination angle was dependent on combining the uncertainties from varying all of the model parameters simultaneously, we found that changing the spectral type of the secondary from a K5 V to an M1 V resulted in a change in the orbital inclination angle of  $1^\circ$ . Similarly, varying  $q$  from 0.030 to 0.056 affected  $i$  by  $\leq 1^\circ$ . We find that the best-fitting  $B$ -,  $V$ -,  $R$ -,  $J$ -,  $H$ -, and  $K_s$ -band model has  $i = 68^\circ$  and the parameters found in Table 3. Figure 1 presents this model for the optical bands, while Figure 2 presents this model for the  $J$ -,  $H$ -, and  $K_s$ -band light curves.

### 3.2. The Model and Its Uncertainties

Based on our optical/IR SED, as well as published values, we adopt a secondary star spectral type of K7 (Torres et al. 2004; McClintock et al. 2001) with a temperature of  $T_{\text{eff}} = 4250$  K (Gray 1992). The corresponding gravity-darkening exponent is  $\beta_1 = 0.34$ .

Modeling six light curves simultaneously is a robust method for constraining the amount of extra light in the system. If we model the light curves individually and assume that all of the light in the system comes from the secondary star, the best-fitting orbital inclination angle for XTE J1118+480 varies with wavelength. Since the contaminating light does not have the same spectrum as the secondary star, the light curves at each wavelength are diluted by different amounts, causing the best-fit inclination for the affected bands to be different from the others. This is the case for the  $B$ - and  $V$ -band light curves. If a jet or other contaminant were to have a flat spectrum that only affected the IR, the results from the SED would most likely not match those obtained from spectral measurements, and we would not be able to determine a reasonable parameter set and inclination angle that is consistent throughout the data. When fit simultaneously, the best-fit inclination angle is  $i = 68^\circ$ , with 62% disk light in  $B$  and 31% disk light in  $V$ . These disk light contributions are consistent with those found through the SED fitting.

TABLE 3  
DERIVED PARAMETERS FOR XTE J1118+480

Parameter	Value
Amount of disk light at $B$ (%).....	$62 \pm 3$
Amount of disk light at $V$ (%).....	$31 \pm 3$
Orbital inclination angle (deg).....	$68 \pm 2$
Primary object mass $M_1$ ( $M_\odot$ ).....	$8.53 \pm 0.60$
Secondary star mass $M_2$ ( $M_\odot$ ).....	$0.37 \pm 0.03$
Orbital separation $a$ ( $R_\odot$ ).....	$2.67 \pm 0.06$
Secondary star radius $R_{L_2}$ ( $R_\odot$ ).....	$0.43 \pm 0.01$
Distance (kpc).....	$1.72 \pm 0.10$

NOTE.—Table errors are  $1\sigma$  ( $\Delta\chi^2 = 1$ ).

Using an estimate of 8% for the infrared accretion disk contamination in the system gives an inclination of  $68_{-2}^{+2.8}$  degrees, however, if we artificially add in 8% or more infrared light, we are unable to obtain a reasonable solution for the orbital inclination angle that is consistent throughout the entire data set. Therefore, based on the IR colors of the system ( $J - K = 1.1 \pm 0.3$ ), the SED fit, and the results of the simultaneous light curve modeling, it appears unlikely that the infrared light curves are significantly affected by any such contamination. In order to determine the final error on the orbital inclination angle, we plotted the  $\chi^2$  values as a function of  $i$ . Therefore, based on the error in each of the model parameters including  $q$ , the spectral type (i.e., temperature) of the secondary star, the amount of observed disk light, and the photometric error bars, the orbital inclination angle is  $68^\circ \pm 2^\circ$ . We combined the determined inclination angle with the orbital period ( $P = 0.1699167 \pm 1.72 \times 10^{-5}$  days), radial velocity of the secondary star ( $K_2 = 709 \pm 7$  km; Torres et al. 2004), and the mass ratio ( $q = 0.0435 \pm 0.0100$ ) to find the mass of the primary object. A Monte Carlo routine was used to propagate the errors on the above quantities and gives a primary mass of  $8.53 \pm 0.60 M_\odot$ , confirming it as a black hole.

The constraints on the mass of the black hole in this system presented here represent a considerable improvement over those previously published. Wagner et al. (2001) determined a mass of  $6.0\text{--}7.7 M_\odot$  from data obtained before XTE 1118+480 had entered a quiescent state ( $R \sim 18.3$  mag). McClintock et al. (2001) gave an upper limit of  $M_1 \leq 10 M_\odot$ , and more recently, McClintock et al. (2004) adopted a mass of  $\sim 8 M_\odot$  for their calculations of the thermal emission from the black hole in the system. The  $8.53 M_\odot$  black hole mass determined here is consistent with the adopted mass of McClintock et al. (2004), and falls nicely into the current observed black hole mass distribution. Theoretical models by Fryer & Kalogera (2001) predict that there should exist a greater number of  $3\text{--}5 M_\odot$  black holes than  $5\text{--}12 M_\odot$  black holes; however, most of the determined black hole masses thus far have fallen into a  $6\text{--}14 M_\odot$  range. In fact, thus far, GRO J0422+32 is the only system with a compact object that falls into the  $3\text{--}5 M_\odot$  range ( $3.97 \pm 0.95 M_\odot$ ; Gelino & Harrison 2003).

Using the mass of the compact object and the orbital period, we computed the orbital separation of the two components in the system. We then combined the separation with the mass ratio to find the size of the Roche lobe for the secondary star. The temperature of the secondary and its Roche lobe radius were then used to find the secondary's bolometric luminosity and bolometric absolute magnitude. After accounting for the bolometric correction (Bessell 1991), the distance modulus for the  $J$ ,  $H$ , and  $K_s$  bands were used to find an average distance of  $1.72 \pm 0.10$  kpc. Consistent with results from the modeling and SED

fitting, this calculation assumes that all of the IR light in the system originates from the secondary star. Table 3 lists all of the derived parameters for the XTE J1118+480 system. Both the mass and radius of the secondary star are smaller than that of a K7 V zero-age main-sequence (ZAMS) star. In addition, the infrared colors of the system and its position in the Galactic halo, support the notion that the secondary star in the XTE J1118+480 system may be evolved.

#### 4. SUMMARY

In this paper, we have presented the first observed *H*- and *K*-band ellipsoidal variations, as well as the first *B*-, *V*-, and *R*-band ellipsoidal variations observed while XTE J1118+480 was in a truly quiescent state. The derived parameters in Table 3 are based on the modeling of these variations including disk contributions of 62% in the *B* band and 31% in the *V* band. Consistent with Shahbaz et al. (2005) and Fitzgerald & Orosz (2003), we do not see evidence for any optical superhump light or irradiation in the system. This supports the interpretation that the system was in a truly quiescent state during our observations.

While the orbital inclination angle found here is lower than that found by groups who optically studied the system while it was approaching quiescence and exhibiting superhumps ( $i = 71^\circ - 82^\circ$ ; Zurita et al. 2002b), it is consistent with that found from

data taken in true quiescence that suggest no significant superhump activity ( $i = 63-73^\circ$ ; Fitzgerald & Orosz 2003). Furthermore, the distance we find is consistent with those found previously through both optical ( $1.9 \pm 0.4$  kpc, Wagner et al. 2001;  $1.8 \pm 0.6$  kpc, McClintock et al. 2001) and infrared ( $1.4 \pm 0.2$  kpc, Mikolajewska et al. 2005) observations.

Simultaneously modeling multiwavelength light curves allows us to better constrain the amount of disk light in an X-ray binary system. As a result, we have been able to constrain the mass of the black hole in the XTE 1118+480 system to  $8.53 \pm 0.60 M_\odot$ , and the distance to the system of  $1.72 \pm 0.10$  kpc.

S. B. acknowledges support from the Turkish Academy of Sciences TUBA-GEBIP (Distinguished Young Scientist) Fellowship. E. K. acknowledges partial support from TÜBİTAK. U. K. and S. B. acknowledge the Turkish National Observatory of TÜBİTAK for providing the facilities for the optical observations. This publication makes use of data products from the Two Micron All Sky Survey, which is a joint project of the University of Massachusetts and the Infrared Processing and Analysis Center/California Institute of Technology, funded by the National Aeronautics and Space Administration and the National Science Foundation.

#### REFERENCES

- Bessell, M. S. 1991, *AJ*, 101, 662  
 Bessell, M. S., & Brett, J. M. 1988, *PASP*, 100, 1134  
 Charles, P. A., & Coe, M. J. 2006 in *Compact Stellar X-Ray Sources*, ed. W.H.G. Lewin & M. van der Klis (Cambridge: Cambridge University Press), in press (astro-ph/0308020)  
 Chen, W., Shrader, C. R., & Livio, M. 1997, *ApJ*, 491, 312  
 Claret, A. 2000, *A&A*, 359, 289  
 Fitzgerald, J. B., & Orosz, J. A. 2003, *BAAS*, 202, 6.01  
 Fryer, C. L., & Kalogera, V. 2001, *ApJ*, 554, 548  
 Garcia, M., Brown, W., Pahre, M., McClintock, J., Callanan, P., & Garnavich, P. 2000, *IAU Circ.*, 7392, 2  
 Garcia, M. R., McClintock, J. E., Narayan, R., Callanan, P., Barret, D., & Murray, S. S. 2001, *ApJ*, 553, L47  
 Gelino, D. M. 2001, Ph.D. thesis, New Mexico State Univ.  
 Gelino, D. M., & Harrison, T. E. 2003, *ApJ*, 599, 1254  
 Gelino, D. M., Harrison, T. E., & McNamara, B. J. 2001a, *AJ*, 122, 971  
 Gelino, D. M., Harrison, T. E., & Orosz, J. A. 2001b, *AJ*, 122, 2668  
 Gray, D. F. 1992, *The Observations and Analysis of Stellar Photospheres* (New York: Cambridge Univ. Press)  
 Harlaftis, E. T., Collier, S., Home, K., & Filippenko, A. V. 1999, *A&A*, 341, 491  
 Hunt, L. K., Mannucci, F., Testi, L., Migliorini, S., Stanga, R. M., Baffa, C., Lisi, F., & Vanzi, L. 1998, *AJ*, 115, 2594  
 McClintock, J. E., Garcia, M. R., Caldwell, N., Falco, E. E., Garnavich, P. M., & Zhao, P. 2001, *ApJ*, 551, L147  
 McClintock, J. E., Narayan, R., Garcia, M. R., Orosz, J. A., Remillard, R. A., & Murray, S. S. 2003, *ApJ*, 593, 435  
 McClintock, J. E., Narayan, R., & Rybicki, G. B. 2004, *ApJ*, 615, 402  
 Mikami, T., & Heck, A. 1982, *PASJ*, 34, 529  
 Mikolajewska, J., Rutkowski, A., Goncalves, D., & Szostek, A. 2005, *MNRAS*, 362, L13  
 Orosz, J. A. 2001, *Astron. Tel.*, 67, 1  
 Remillard, R., Morgan, E., Smith, D., & Smith, E. 2000, *IAU Circ.*, 7389, 2  
 Shahbaz, T., Dhillion, V. S., Marsh, T. R., Casares, J., Zurita, C., Charles, P. A., Haswell, C. A., & Hynes, R. I. 2005, *MNRAS*, 362, 975  
 Stetson, P. B. 1987, *PASP*, 99, 191  
 Torres, M. A. P., Callanan, P. J., Garcia, M. R., Zhao, P., Laycock, S., & Kong, A. K. H. 2004, *ApJ*, 612, 1026  
 van Hamme, W. 1993, *AJ*, 106, 2096  
 Wagner, R. M., Foltz, C. B., Shahbaz, T., Casares, J., Charles, P. A., Starrfield, S. G., & Hewett, P. 2001, *ApJ*, 556, 42  
 Wijnands, R. 2005, in *Progress in Neutron Star Research*, ed. A. P. Wass (Hauppauge: Nova Science)  
 Wilson, R. E. 1998, in *Reference Manual to the Wilson-Devinney Program, Computing Binary Star Observables, Version 1998* (Gainesville: Univ. Florida)  
 Yuan, F., & Cui, W. 2005, *ApJ*, 629, 408  
 Zurita, C., Casares, J., Martinez-Pais, I. G., Piccioni, A., Bernabei, S., Bartolini, C., & Guarnieri, A. 2002a, *IAU Circ.*, 7868, 1  
 Zurita, C., Casares, J., Shahbaz, T., Wagner, R. M., Foltz, C. B., Rodriguez-Gil, P., Hynes, R. I., Charles, P. A., Ryan, E., Schwarz, G., & Starrfield, S. G. 2002b, *MNRAS*, 333, 791